Ultrametricity of optimal transport substates for multiple interacting paths over a square lattice network

Marco Cogoni,* Giovanni Busonera,† and Gianluigi Zanetti‡
CRS4: Center for Advanced Studies, Research and Development in Sardinia - 09010 Pula (CA), Italy
(Dated: November 16, 2016)

We model a set of point-to-point transports on a network as a system of polydisperse interacting self-avoiding walks (SAWs) over a finite square lattice. The ends of each SAW may be located both at random, uniformly distributed, positions or with one end fixed at a lattice corner. The total energy of the system is computed as the sum over all SAWs, which may represent either the time needed to complete the transport over the network, or the resources needed to build the networking infrastructure. We focus especially on the second aspect by assigning a concave cost function to each site to encourage path overlap. A Simulated Annealing optimization, based on a modified BFACF Montecarlo algorithm developed for polymers, is used to probe the complex conformational substates structure. We characterize the average cost gains (and path-length variation) for increasing polymer density with respect to a Dijkstra routing and find a non-monotonic behavior as previously found in random networks. We observe the expected phase transition when switching from a convex to a concave cost function (e.g., x^γ, where x represents the node overlap) and the emergence of ergodicity breaking, finally we show that the space of ground states for $\gamma < 1$ is compatible with an ultrametric structure as seen in many complex systems such as some spin glasses.

arXiv:1611.04918v1 [cond-mat.stat-mech] 15 Nov 2016

The problem of optimal transport over various kinds of networks is important both for theoretical and practical reasons [1]. Areas of application range from river networks [2, 3] to vascular systems in animals and plants [4, 5], and from electric energy distribution systems [6] to communication networks [7, 14]. The adoption of a cost function minimization scheme has allowed a unified approach to very diverse research fields. Cost functions may be thought as energy dissipation for electricity grids, time delay and/or resources needed to build the networking infrastructure. In recent years, the relation between the properties of the cost function and the associated optimal solutions has been extensively studied [7]. For instance, when multiple sources are connected to a single destination (as in drainage basins), it is known that a concave cost leads to multiple (nearly equivalent) spanning trees, whereas a convex behavior shows a unique redundant solution with many loops. When the character of the cost function is not well defined, no *a priori* conclusions may be drawn [8].

It is well known [7] that, for concave cost functions, a multiplicity of local optimal solutions exists. Since a hierarchical organization of the states is observed, one may hypothesize an ultrametric relation among them. Ultrametricity (UM) is one of the key features of the mean-field Parisi picture for spin glasses[9]: the states of the system obey an UM distance which translates into a hierarchical organization. This behavior has been hypothesized or observed for different polymer systems with noise, such as directed polymers in random media (DPRM) [10–12] and for self-interacting SAWs in external fields [13]. Our model has three main differences with respect to the DPRM formulation: 1) the (locally) minimum cost is achieved by collectively optimizing several interacting chains; 2) polymers are polydisperse and have at least one end which is randomly located on the lattice meaning that quenched disorder is achieved through random topology rather than noisy bonds; 3) our polymers may not be directed: they are free to wander backwards/sideways to achieve a global cost gain. This behavior is seldom observed for weakly interacting polymers or very dilute system.

In this paper we show a non-monotonic behavior of the optimized cost gain, with respect to a Dijkstra routing, when increasing polymer density as previously found for random networks [14]. Moreover, we observe the emergence, for concave costs, of ergodicity breaking and present evidence that the space of ground states for is compatible with an ultrametric structure.

Model and Numerical Methods – We consider a square lattice network of $N = L^2$ nodes and side L, each node connected to its four nearest neighbors via uniform links with adjacency matrix $A_{ij} = A_{ji} = 1$, zero elsewhere. A set of M communications, modeled as polymers with fixed ends, compete on the network for the available resources, each occupying a path described by an interacting SAW. The self-avoidance condition enforces that no path uses the same node more than once, whereas distinct polymers can use the same node. The occupation number of each path ν on the node i is denoted by $\sigma_i^\nu \in \{0, 1\}$. The total occupation number on the i-th node is $I_i = \sum_\nu \sigma_i^\nu$. The interaction among polymers is regulated by a Hamiltonian of the form

$$H = M \sum_i f(k_i \frac{I_i}{M})$$

where the concave/convex character of the cost function f makes the system behave in qualitatively different ways [7]. The occupation number is normalized by M in order to have a uniform temperature behavior with re-

spect to polymer multiplicity. The k_i are node-dependent weights, in general set to unity, which may be used to model non-uniformity by adding some noise. In this paper we consider only the simplest functional form for the cost f: the power function $f(x) = x^\gamma$. This functional dependence leads to polymer repulsion for $\gamma > 1$, whereas $\gamma < 1$ encourages overlap. For $\gamma = 1$ the polymers do not interact, and it is known that the ground state of H is attained by (highly degenerate) shortest-path routing [7, 14].

To explore the energy landscape of H for $\gamma \neq 1$, we adopt a Simulated Annealing (SA) scheme in which temperature is gradually decreased within a canonical Montecarlo (MC). The basic MC move follows the BFACF algorithm developed for lattice polymers [15, 16]. With respect to the original scheme, at each iteration one polymer is randomly selected and instead of applying the basic move at a single random site, we perform multiple moves. The number of moves on the SAW is randomly chosen within one and the average polymer length. This random choice of basic move multiplicity guarantees good MC acceptance rates [17]. Since in this work we are dealing with several interacting polymers, we rely on the Gibbs acceptation factor of the MC to extract a chain of states from the canonical ensemble instead of direct generation as in Ref. [15]. Assigning the same probability both to path-enlarging and path-shrinking BFACF moves leads to very low acceptance rates. We solve this problem by tying the probability of path-enlarging moves to the MC temperature [18].

The square lattice with uniform $k_i = 1$ factors induces on this problem some peculiarities not found in a continuous representation of space. In particular, the ground states for basic routing problems (i.e., involving non-interacting polymers) in two dimensions are intrinsically degenerate because $\binom{m+n}{n}$ solutions with the same energy exist between any pair of points with m horizontal and n vertical distance [19].

We restrict our study to two-dimensional lattices with no periodic boundary conditions (PBC) to better model realistic network topologies. Preliminary numerical results show that qualitatively similar conclusions may be drawn when PBC are imposed at the boundaries.

Detecting UM in finite-volume systems can be very difficult due to finite-size effects especially in the present case for which PBC are not applied [20–24]. To measure differences between replicas α, β for the same quenched disorder, we define a path overlap $q_{\alpha\beta}$, computed as the ratio of the common visited nodes (node-overlap $\dot{q}_{\alpha\beta}$) or common visited links (link-overlap $\tilde{q}_{\alpha\beta}$) with respect to path length [25]. For homologue SAWs α, ν and β, ν, we define the node overlap as

$$\dot{q}^\nu_{\alpha\beta} = \frac{1}{N_{nodes}} \sum_i \sigma_i^{\alpha,\nu} \sigma_i^{\beta,\nu}$$

and the link overlap

$$\tilde{q}^\nu_{\alpha\beta} = \frac{1}{N_{links}} \sum_{i,j} A_{ij} \sigma_i^{\alpha,\nu} \sigma_j^{\alpha,\nu} \sigma_i^{\beta,\nu} \sigma_j^{\beta,\nu}.$$

From the overlap we get the normalized Hamming distance as $\delta_{\alpha\beta} = 1 - q_{\alpha\beta}$. The two different overlap measures give compatible results, but the data shown in this paper is computed by using the link-overlap $\tilde{q}_{\alpha\beta}$.

In an UM space [20] the triangle inequality $\delta_{\alpha\gamma} \leq \delta_{\alpha\beta} + \delta_{\beta\gamma}$ valid for metric spaces, is replaced by a stronger version $\delta_{\alpha\gamma} \leq max\{\delta_{\alpha\beta}, \delta_{\beta\gamma}\}$. This inequality is equivalent to imposing that any triple of points should form an acute isosceles triangle or, at most, an equilateral one. In order to discern between trivial UM due to equilateral triangles or true UM due to acute isosceles ones, we perform a further test in which we analyze the frequency distribution of each triple of ordered distances $\delta_{max}, \delta_{med}, \delta_{min}$, by plotting only two transformed components as defined in Ref.[26]: $Y = \delta_{max} - \delta_{med}$ vs $X = \delta_{med} - \delta_{min}$.

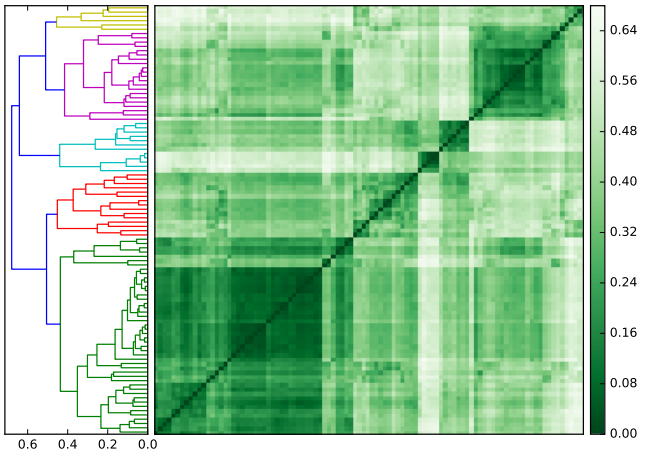

FIG. 1. Dendrogram and distance matrix for 100 states for $N = 1024, M = 64$ and $\gamma = 0.5$. Each matrix element represents the Hamming distance (normalized by path length) for one of the M homologue SAWs belonging to each pair of states.

We compute the distance $\delta_{\alpha\beta}$ for all pairs of states with the same quenched disorder. This is achieved by selecting pairs of homologue SAWs belonging to the two states α and β, and finally computing their Hamming distance (normalized by path length.)By applying a clustering algorithm to each disorder, we obtain a dendrogram such as the one in the left part of Fig. 1, where a deep hierarchical structure is qualitatively visible. We then sort all states in the same order as the dendrogram and plot the adjacency matrix: a well-visible block-diagonal complex structure emerges for $\gamma = 0.5$. On the other hand, a flat hierarchy is observed for $\gamma \geq 1$ when no noise is applied. The clustering of states and their adjacency matrix have been obtained by following an approach similar to Refs. [21, 22, 24]. To probe for an UM space structure, we

randomly select three configurations from the hierarchical cluster structure (see Ref. [21]), resulting in three mutual distances. After sorting we get $\delta_{max} \geq \delta_{med} \geq \delta_{min}$ and compute the correlator $K = \frac{\delta_{max} - \delta_{med}}{\delta_{min}}$. If the phase space is UM, we expect $\delta_{max} = \delta_{med}$ for $L \to \infty$. Thus $P(K)$ should converge to a delta function in $K = 0$ for $L \to \infty$ and the variance of the distribution $Var(K) \to 0$. By this approach, UM would be detected even in the case of equilateral triangles (trivial UM). The alternative definition of K in Ref. [22] is difficult to apply for polydisperse SAWs (each SAW length has a distinct distance distribution), so we devised a supplementary test to rule out trivial UM.

Results and discussion – All ground states have been obtained by performing a SA energy minimization with an exponential cooling converging to $T = 0$ at one third of the total simulation length. To characterize cost gain and path-length variation for the system with both random ends, we performed several minimizations in which the number of SA timesteps varied with system size from $0.5 \cdot 10^6$ for $L = 8$ and $M = 8$ to $10 \cdot 10^6$ for $L = 64$ and $M = 1024$. The maximum number of basic BFACF moves per timestep was proportional to $\sqrt{N}$. For each lattice size we generated 10 quenched disorders with random uniform configurations and for each disorder we produced 10^2 local ground states. We plan to expand this number for future works.

The first goal was to characterize the system as regards the attainable cost gain with respect to the shortest path routing which is widely used for many transport applications. In Fig. 2 we plot the energy difference ratio both for concave ($\gamma < 1$, continuous blue online) and convex ($\gamma > 1$, dashed red online) cost functions .

Since the average polymer length increases with L, we observe in Fig. 2 the tendency of the curves to superimpose for $N \to \infty$. The peaks are shifted for $\gamma < 1$ and $\gamma > 1$: $M/\sqrt{(N)} \sim 1$ and ~ 2, respectively. After a steep cost gain growth, maximum efficiency with respect to Dijkstra is reached for both γ values, then the value slowly decreases since most nodes are already busy and the advantage of longer-than-Dijkstra detours is weaker. Cost gain ratios are quite different for $\gamma < 1$ and $\gamma > 1$: for the convex case, the gain ratio is relatively constant for any M at nearly 40%, while in the concave situation, it rarely goes beyond 20% and decreases more markedly for higher M values. By comparing the peak values of Fig. 2 with their associated path-length variations in Fig. 3, we can verify that large cost gains may be obtained by employing slightly longer paths (always $< 2\%$ for both γ values.) These results are qualitatively very similar to those obtained by a cavity optimization approach in Ref. [8, 14] for random paths on a random graph with constant connectivity $k = 3$. It should be stressed that the regular lattice is not tractable with the cavity method since too many loops exist, leading to severe ground state degeneration. The present method may be exploited to minimize networking resources thus obtaining a compact network (sparse subset of the lattice for $\gamma < 1$) and then selecting/modifying the ground states with sufficient transport performance when $\gamma > 1$.

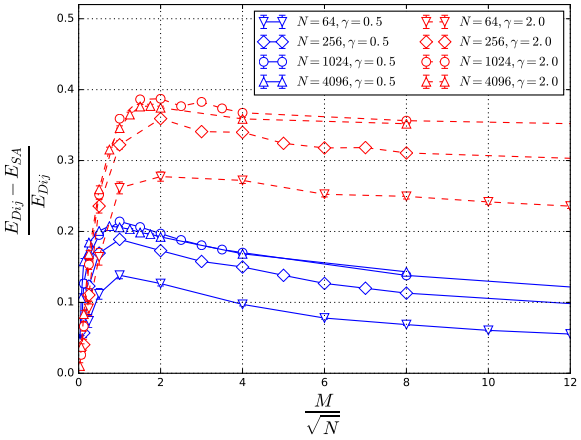

FIG. 2. Cost decrease ratio of the SA with respect to a Dijkstra algorithm.

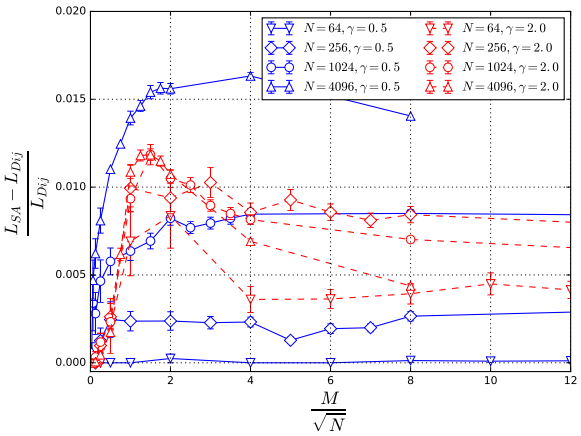

FIG. 3. Path length increase ratio for the SA with respect to a Dijkstra algorithm.

Let us focus for the rest of the paper on the concave cost case. In the Supplementary Materials to Ref. [14], there is a brief discussion regarding the possibility of a RSB scenario for $\gamma < 1$. This led us to question whether an UM structure among the ground states of our closely related system exists. We consider two polymer distributions: one in which both SAW ends are uniformly distributed over the lattice and another in which one end is constrained to a corner of the lattice. It has become customary to show a tendency towards UM by plotting the distribution $P(K)$ for several system sizes along with its variance $Var(K)$. In Fig. 4 the $P(K)$ for the random-ends polymers (top) and for the fixed-end polymers (bottom) are shown. There is a visible trend of both $P(K)$ to

diverge for $K \to 0$ when $N \to \infty$. Both polymer topologies share the same overall behavior. In the two insets of Fig. 4(top and bottom) we can compare the variance of the $P(K)$ for both systems compared to their randomized counterparts [27]: they both tend to zero as lattice size grows, so we cannot still conclude in which case whether UM is attained in the infinite-size limit. In Fig. 5 we can see the details of the distributions for the distance triples for one randomized configuration and three lattice sizes of the fixed end polymer system. The randomized system shows that the majority of (X, Y) points lie very near the origin where equilateral triangles reside. On the contrary, the optimized polymer systems all show a larger concentration towards the X axis which corresponds to the acute isosceles triangles of true UM. This is better shown by the white circles representing the center of mass for each distribution: with respect to the randomized state, in which the center-of-mass approaches the origin with $N \to \infty$, the optimized states tend to stay nearer to the X-axis without converging to the origin.

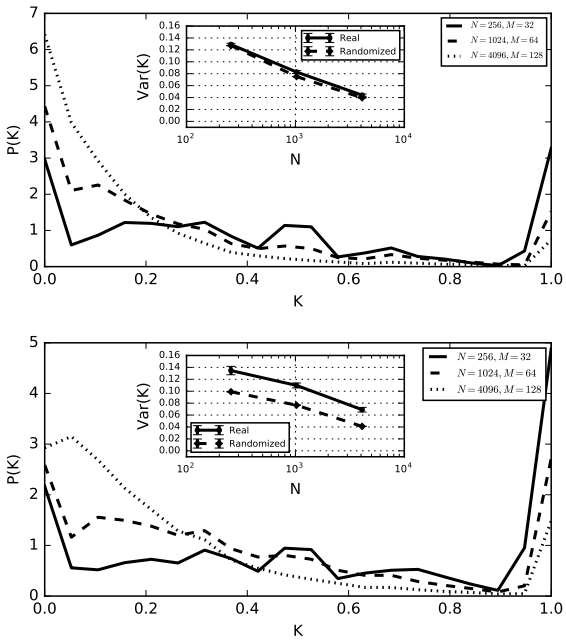

FIG. 4. Distribution $P(K)$ for different N and polymer number $M = 2\sqrt{N}$. Top graph refers to the unconstrained polymers, while bottom to the corner constrained case. Collinear triangles ($K \approx 1$) tend to disappear with growing N for both systems.

Conclusions – In the present letter we presented a novel approach to explore the ground states of an important class of transport optimization problems on a regular square lattice. We showed that with this method one is able to obtain solutions for the optimal transport of a set of interacting communications spread over the lattice with different topological constraints. The interaction among paths is obtained within the unifying framework of concave/convex cost functions. The fact that this method works on a lattice, allows the possibility of discovering a hierarchy of the most inexpensive network infrastructures encouraging transport coalescence ($\gamma < 1$) and then to optimize the distilled graph for performance, fault tolerance and congestion resistance with a repulsive cost function ($\gamma > 1$) as in Ref. [14]. We tested our optimization procedure by characterizing the global cost gain and path-length variation for a system of randomly spread point-to-point communications over a square lattice that has been recently studied on random graphs via the cavity method [14] obtaining qualitatively similar results. The appearance of families of hierarchically related solutions led us to verify whether an UM structure exists. Similarities and differences with respect to spin systems allowed us to borrow a standard approach to probe for UM, which we slightly extended by plotting the distribution of triangle types for growing lattice sizes. In conclusion we found evidence supporting UM at the level of single interacting polymers as hypothesized for DPRM systems [10]. Here the equivalent of noise (highly correlated) is apparently played by all polymers minimizing the total energy so forming a rough landscape [28, 29]. It should be further investigated whether and how this phenomenon depends on polymer density/dispersity and γ values. Finally, we plan to further investigate if a global similarity measure, encompassing all SAWs, can be defined to assess whether an UM structure exists at the system level.

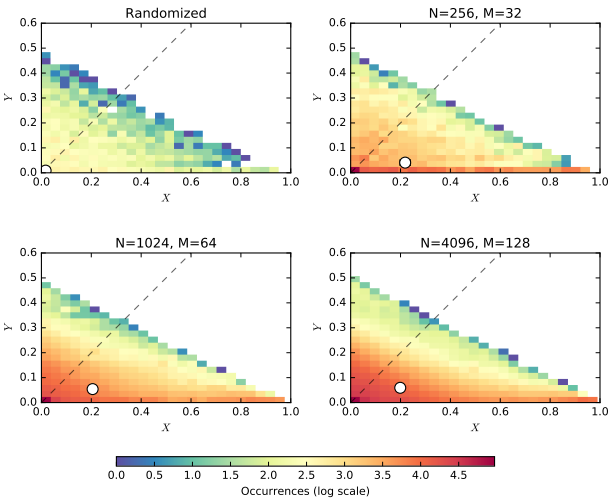

FIG. 5. Corner-constrained polymers: For every triplet of distances (among homologue SAWs) we plot the distributions of points (X, Y). Top panels refer respectively to the randomized paths (left) for $N = 256, M = 32$ and its center of mass lying at the origin (i.e., trivial UM) while on the right the center of mass shifts to $X \sim 0.2$ and $Y \to 0$. Increasing lattice size (bottom panels), a large fraction of triangles lie near the X-axis (acute isosceles triangles). A similar result holds for the unconstrained polymers (not shown.)

We thank Francesco Versaci for useful discussions.

* marco.cogoni@crs4.it
† giovanni.busonera@crs4.it
‡ gianluigi.zanetti@crs4.it

[1] A. B. Jayanth R, M. Amos, and Rinaldo, Nature **399**, 130 (1999).
[2] A. Rinaldo, R. Rigon, J. R. Banavar, A. Maritan, and I. Rodriguez-Iturbe, Proceedings of the National Academy of Sciences of the United States of America **111**, 2417 (2014).
[3] E. J. Ijjász-Vásquez, R. L. Bras, I. Rodríguez-Iturbe, R. Rigon, and A. Rinaldo, Advances in Water Resources **16**, 69 (1993).
[4] E. Katifori, G. J. Szöllosi, and M. O. Magnasco, Physical Review Letters **104**, 048704 (2010), arXiv:0906.0006.
[5] F. Corson, Physical Review Letters **104**, 048703 (2010), arXiv:0905.4947.
[6] S. Bohn and M. O. Magnasco, Physical Review Letters **98**, 088702 (2007), arXiv:0607819 [cond-mat].
[7] J. R. Banavar, F. Colaiori, A. Flammini, A. Maritan, and A. Rinaldo, Physical Review Letters **84**, 4745 (2000).
[8] C. H. Yeung and D. Saad, Physical Review Letters **108**, 208701 (2012), arXiv:1202.0213.
[9] M. Mezard, G. Parisi, and M. Virasoro, *Spin Glass Theory and Beyond*, Lecture Notes in Physics Series (World Scientific, 1987).
[10] Y.-C. Zhang, Phys. Rev. Lett. **59**, 2125 (1987).
[11] M. Kardar and Y. C. Zhang, Physical Review Letters **58**, 2087 (1987).
[12] N.-N. Pang and T. Halpin-Healy, Phys. Rev. E **47**, R784 (1993).
[13] A. Fernández, International Journal of Theoretical Physics **30**, 83 (1991).
[14] C. H. Yeung, D. Saad, and K. Y. M. Wong, Proceedings of the National Academy of Sciences of the United States of America **110**, 13717 (2013), arXiv:arXiv:1309.0745v1.
[15] B. Berg and D. Foerster, Physics Letters B **106**, 323 (1981).
[16] C. Aragão de Carvalho and S. Caracciolo, J. Phys. France **44**, 323 (1983).
[17] C. Sergio, P. Andrea, and S. Alan, Journal of Statistical Physics **60**, 1 (1990).
[18] K. Binder, *Monte Carlo and Molecular Dynamics Simulations in Polymer Science* (Oxford University Press, 1995).
[19] L. Mernik, J. of Pure and Applied Math **56**, 589 (2009).
[20] R. Rammal, G. Toulouse, and M. A. Virasoro, Reviews of Modern Physics **58**, 765 (1986).
[21] G. Hed, A. P. Young, and E. Domany, Physical Review Letters **92**, 157201 (2004).
[22] H. G. Katzgraber and A. K. Hartmann, Physical Review Letters **102**, 037207 (2009), arXiv:arXiv:0807.3513v1.
[23] H. G. Katzgraber, T. Jorg, F. Krzakala, and A. K. Hartmann, Physical Review B - Condensed Matter and Materials Physics **86**, 184405 (2012), arXiv:arXiv:1205.4200v1.
[24] S. Ciliberti and E. Marinari, Journal of Statistical Physics **115**, 557 (2004).
[25] Whenever two strings possess different lengths, we concatenate a padding string to the short one.
[26] P. Contucci, C. Giardinà, C. Giberti, G. Parisi, and C. Vernia, Physical Review Letters **99**, 057206 (2007).
[27] The randomized system is obtained by reshuffling every SAW sequence with the same quenched disorder. The randomized paths do maintain legal connection between polymer ends, but self-avoidance may be violated.
[28] S. V. Buldyrev, S. Havlin, and H. E. Stanley, Physical Review E - Statistical, Nonlinear, and Soft Matter Physics **73**, 036128 (2006).
[29] L. A. Braunstein, S. V. Buldyrev, S. Havlin, and H. E. Stanley, Physical Review E - Statistical, Nonlinear, and Soft Matter Physics **65**, 056128 (2002).